# Phase diagrams of hard spheres with algebraic attractive interactions

# Phase diagrams of hard spheres with algebraic attractive interactions

Philip J. Camp*
*School of Chemistry, University of Edinburgh, West Mains Road, Edinburgh EH9 3JJ, United Kingdom*
(Received 15 August 2002; published 17 January 2003)

The phase diagrams of systems made up of hard spheres interacting with attractive potentials of the form $-1/r^{3+\sigma}$ are calculated using Monte Carlo simulations, second-order thermodynamic perturbation theory, and an augmented van der Waals theory. In simulations of the systems with $\sigma=0.1$, 1, and 3, fluid-solid coexistence results are obtained using the Gibbs-Duhem integration technique; simulation data for the vapor-liquid coexistence envelopes and critical points are taken from previously published work [P. J. Camp and G. N. Patey, J. Chem. Phys. **114**, 399 (2001)]. It is shown that the agreement between the theoretical and simulated phase diagrams improves as the range of the potential is increased, reflecting the decreasing role of short-range correlations in determining the bulk thermodynamics. In the extreme case of $\sigma=0.1$ both theories are in excellent agreement with simulations. Phase diagrams for systems with $\sigma=4$, 5, and 6 are computed using second-order thermodynamic perturbation theory. The results indicate that the vapor-liquid transition becomes metastable with respect to freezing when $\sigma\gtrsim 5$, in broad agreement with results for the hard-sphere attractive Yukawa system which is commonly used to model colloidal particles, globular proteins, and nanoparticles.

DOI: 10.1103/PhysRevE.67.011503 PACS number(s): 64.70.Fx, 64.10.+h, 64.70.Dv

## I. INTRODUCTION

The thermodynamic behavior of systems made up of particles interacting with long-range potentials has long been a topic of interest in condensed-matter science. In effect, van der Waals' eponymous equation of state was derived by assuming that the molecules in a fluid interact with uniform weakly attractive potentials. Such models have provided a valuable insight into the physical mechanisms that give rise to phase separation in fluids, but they fail to describe accurately the vapor-liquid critical regions of real fluids. Most one-component three-dimensional fluids possess interactions which are ''short ranged'' (to be defined below), and the corresponding vapor-liquid critical exponents take on universal (Ising) exponents. For example, the difference between vapor and liquid coexistence densities on approach to the critical temperature $T_c$ from below scales like $|T_c-T|^{\beta}$, where the Ising exponent is $\beta=0.326(4)$ [1]. In contrast, the van der Waals equation of state predicts the mean-field value $\beta=\frac{1}{2}$. Nonetheless, almost a century after van der Waals' seminal work, vapor-liquid criticality and magnetic criticality were predicted theoretically to belong to the mean-field universality class, provided the interactions operating between the particles or spins are sufficiently long ranged [2–6]. Indeed, if the intermolecular pair potential varies with the separation $r$ like $-1/r^{3+\sigma}$, with $\sigma>0$, then three regimes of critical behavior for the system in $D$ dimensions can be identified: (i) the short-range regime $\sigma>2-\eta_{\rm sr}$ exhibiting Ising-like criticality; $\eta_{\rm sr}$ is the Ising value of the correlation decay exponent, which in three dimensions has the value $0.0335\pm 0.0025$ [7]; (ii) the long-range regime $\sigma<D/2$ for which the criticality is mean field; (iii) the intermediate-range regime $D/2<\sigma<2-\eta_{\rm sr}$ in which the criticality interpolates linearly between the short-range and long-range regimes [8]. These regimes have been studied in detail in recent simulations of lattice models with attractive interactions proportional to $-1/r^{3+\sigma}$ [9,8].

Recently, vapor-liquid criticality in hard-sphere systems with long-range attractive potentials was studied using mixed-field finite-size scaling simulations [10]. The intermolecular potential studied in this work was of the form

$$v(r)=v_0(r)+v_1(r), \tag{1}$$

where $v_0(r)$ is the short-range hard-sphere potential, defined by

$$v_0(r)=\begin{cases}\infty & r<d\\ 0 & r\geqslant d,\end{cases} \tag{2}$$

and $v_1(r)$ is the attractive tail, given by

$$v_1(r)=-\epsilon\left(\frac{d}{r}\right)^{3+\sigma}. \tag{3}$$

In Eqs. (2) and (3), $d$ is the hard-sphere diameter, and $\epsilon$ is the potential well depth. When reporting thermodynamic properties of this system, it is convenient to define the following reduced units: the reduced temperature $T^*=k_{\rm B}T/\epsilon$, where $k_{\rm B}$ is Boltzmann's constant and $T$ is the temperature; the reduced inverse temperature $\beta^*=\beta\epsilon=1/T^*$ where $\beta=1/k_{\rm B}T$; the reduced pressure $p^*=pd^3/\epsilon$, where $p$ is the pressure; the reduced number density, $\rho^*=\rho d^3$, where $\rho=N/V$, $N$ is the number of particles, and $V$ is the volume of the system; the reduced energy density, $u^*=u/\epsilon$, where $u=U/N$, and $U$ is the configurational energy.

In Ref. [10] it was shown that with $\sigma=3$ the vapor-liquid critical behavior was entirely consistent with the Ising-like criticality expected in the short-range regime. For long-range potentials with $\sigma=1$ and $\sigma=0.1$, significant deviations from Ising-like criticality were observed. In addition, the relationship between the critical density, critical temperature, and the range parameter $\sigma$ was tested against a prediction made by Brilliantov and Valleau employing a mean-field analysis of the Landau-Ginzburg-Wilson effective Hamiltonian [11]. It

*Email address: philip.camp@ed.ac.uk

 

was seen that the theory becomes more accurate as the range of the potential is increased, indicating the crossover to mean-field criticality. Brilliantov and Valleau first tested their relation against Monte Carlo (MC) simulation results for square-well fluids, with the same conclusion.

To date, studies of off-lattice systems with long-range interactions have largely been restricted to calculating vapor-liquid coexistence and criticality. Mention has already been made of the work by Brilliantov and Valleau on square-well fluids [11], but we might also note the study on the same system by Vega *et al.* [12] in which Gibbs ensemble MC (GEMC) simulations were used to correlate the shape of the vapor-liquid coexistence envelope with the crossover to mean-field criticality as the range of the potential was increased.

One of the aims of this paper is to present complete phase diagrams of systems with long-range interactions calculated using accurate computer simulations, and to assess how well classical, or mean-field, theories perform in comparison. Perhaps the most widely used theoretical approach is the thermodynamic perturbation theory (TPT) of Barker and Henderson [13–15]. TPT provides expressions for the change in Helmholtz free energy of a reference hard-core system in the presence of an attractive intermolecular potential as an expansion in $1/T$. The first-order term $O(1/T)$ can be calculated exactly using the radial distribution function of the reference hard-sphere system, $g_0(r)$. The second-order term $O(1/T^2)$ is given in terms of four-particle correlation functions, but can be approximated in terms of $g_0(r)$ and the isothermal compressibility of the reference system. TPT is expected to be most accurate when the attractive potential varies slowly over distances comparable to the hard-core diameter; in this case the potential can be thought of as providing a roughly uniform attractive background, which does not significantly alter the short-range correlations arising from the hard-core repulsions.

The van der Waals theory corresponds to the limit of a weak uniform attraction between the particles. Widom and Longuet-Higgins showed how an augmented van der Waals theory can be constructed for fluid and solid phases from the knowledge of the reference hard-core system [16–18]. Such a theory is equivalent to calculating the Helmholtz free energy in TPT by evaluating the first-order term $O(1/T)$ with $g_0(r)=1$ for $r>d$, and ignoring higher-order terms. Improvements over the original van der Waals theory arise from treating the hard-core reference system very accurately, and hence the freezing transition can be accommodated within the augmented theory.

With regard to the reference hard-sphere system, the Helmholtz-free energies and equations of state are well known for both the fluid [19] and face-centered cubic (fcc) solid phases [20,21]. The corresponding radial distribution functions, $g_0(r)$, have also been accurately determined [22,23]. In the present work we will not consider the hexagonal close-packed (HCP) phase, which has been found to have a chemical potential only $\sim 10^{-3} k_B T$ higher than that of the FCC solid, close to the melting density [24]. Other crystal lattices can be safely ignored by virtue of having low close-packed densities.

To investigate the phase diagrams of systems with long-range interactions, we have carried out MC computer simulations of the model defined in Eqs. (1)–(3) with $\sigma=0.1$, 1, and 3. We have determined the fluid-solid phase boundaries for each system using the Gibbs-Duhem integration technique devised by Kofke [25]. Simulation data for the vapor-liquid coexistence curves and associated critical parameters were taken from Ref. [10]. We have also computed the equilibrium phase diagrams using second-order thermodynamic perturbation theory (STPT), and an augmented van der Waals theory. We will demonstrate that the agreement between the simulated and theoretical phase diagrams improves as the range of the potential is increased; at $\sigma=0.1$ the accuracies of both theories are essentially quantitative.

The phase behavior of various hard-core systems with very short-range attractive interactions has recently received a great deal of attention because of the relevance to colloidal systems, globular protein crystallization, nanoparticle aggregation, and fullerenes. For example, a widely studied generic model of such materials is the hard-sphere system with attractive Yukawa potentials of the form $v_1(r)=-\epsilon\exp[-\kappa(r-d)](d/r)$, where $\epsilon$ is the attractive well depth, $1/\kappa$ is a length parameter characterizing the range of the potential, and $d$ is the hard-sphere diameter. Hagen and Frenkel found that the vapor-liquid transition becomes metastable with respect to the fluid-fcc-solid transition when $\kappa d \gtrsim 6$ [26], whilst Bolhuis *et al.* showed that the same potential gives rise to an isostructural (fcc) solid-solid transition when $\kappa d \gtrsim 25$ [27]. The phase diagram and formation of glassy phases in this system have recently been studied in detail by Foffi *et al.*, using a combination of TPT, mode-coupling theory, and the self-consistent Ornstein-Zernike approximation [28]. The qualitative features of the attractive Yukawa system have also been found in square-well fluids with very short-range attractions [29,27,28]. Integral equation and TPT approaches are generally quite successful for all of these systems, although first-order TPT has recently been shown to give rise to unphysical phase diagrams for extremely short-range potentials [30].

Relatively little work has been reported on the particular potential defined in Eqs. (1)–(3) with large, but finite, values of $\sigma$, although some equations of state and other thermodynamic properties have been obtained for fluid systems with $3 \leqslant \sigma \leqslant 33$ using computer simulations [31] and STPT [32]. We also note the recent work of Noro *et al.* [33], in which the phase behavior, and in particular the formation of a gel phase, was studied in systems with $\sigma=47$ and a uniform long-range attraction.

For completeness, we will present phase diagrams calculated using STPT for systems with $\sigma=4$, 5, and 6, which show that the vapor-liquid critical temperature drops below the triple point temperature when $\sigma \gtrsim 5$, whereupon condensation becomes metastable with respect to freezing. The effective range of the potential with $\sigma=5$ is comparable to that for the corresponding attractive Yukawa potential with $\kappa d=6$ [26].

This paper is organized as follows. The simulation techniques employed to determine the fluid-solid phase boundaries are described in Sec. II. In Secs. III and IV we summa-

rize the STPT and augmented van der Waals theories, respectively. The results are presented in Sec. V, and Sec. VI concludes the paper.

## II. COMPUTER SIMULATIONS

Isothermal-isobaric MC ($NpT$-MC) simulations were performed on systems with $N=256$ particles in a cubic simulation cell of dimension $L$, with periodic boundary conditions applied [34]. The attractive part of the potential, $v_1(r)$, was truncated at $r_{\rm cut}=L/2$; pair interactions were evaluated using the minimum image convention. The long-range contribution to the total energy, $U_{\rm LR}$, was estimated in the usual way by assuming $g(r)=1$ for $r \geqslant r_{\rm cut}$,

$$U_{\rm LR}=2\pi N\rho\int_{r_{\rm cut}}^{\infty} r^2 g(r) v_1(r) dr \simeq -\frac{2\pi N\rho^* \epsilon}{\sigma}\cdot\left(\frac{d}{r_{\rm cut}}\right)^{\sigma}. \tag{4}$$

Fluid-solid coexistence was traced using the Gibbs-Duhem integration technique devised by Kofke [25]. We chose to integrate a Clapeyron-type equation that relates the derivative of $\beta p$ at coexistence with respect to $\beta$. The Gibbs-Duhem equation for a single-phase one-component system can be written as

$$d(\beta\mu)=u d\beta+(1/\rho)d(\beta p), \tag{5}$$

where $\mu$ is the chemical potential. For two phases, labeled 1 and 2, to be at coexistence at given reciprocal temperature and pressure, we have the condition $\mu_1=\mu_2$. If the reciprocal temperature is altered by an infinitesimal amount, $d\beta$, then for coexistence to be maintained, the pressure must be adjusted such that

$$d(\beta\mu_1)=d(\beta\mu_2). \tag{6}$$

Substituting Eq. (5) into Eq. (6) yields a Clapeyron-type differential equation describing the change in $\beta p$ at coexistence in response to a change in reciprocal temperature,

$$\frac{d\beta p}{d\beta}=-\left(\frac{u_2-u_1}{1/\rho_2-1/\rho_1}\right). \tag{7}$$

The integration was performed using simulation data for the rhs (right-hand side) of Eq. (7), starting from $\beta^*=0$ at which the fluid-solid transition coincides with that of hard spheres (the solid phase is assumed fcc throughout). The coexistence data for the hard-sphere fluid-solid transition in the current simulation units are [35]

$$\beta^* p^*=11.69, \tag{8}$$

$$\rho^*_{\rm fluid}=0.943, \tag{9}$$

$$\rho^*_{\rm solid}=1.041. \tag{10}$$

In practice, for each system we first carried out the integration scheme as originally proposed by Kofke [25], i.e., by using a predictor-corrector technique. The interval in reciprocal temperature, $\delta\beta^*$, used for the integration depended on the system. For $\sigma=0.1$ we used $\delta\beta^*=0.01$, whilst for $\sigma=1$ and $\sigma=3$ we used $\delta\beta^*=0.1$. Upon completing a numerical integration between the initial and final temperatures, we fitted the rhs of Eq. (7) (in simulation units) to a cubic polynomial in $\beta^*$, from which the function $\beta^* p^*(\beta^*)$ was obtained by analytic integration,

$$\frac{d\beta^* p^*}{d\beta^*}=\sum_{n=0}^{3} a_n \beta^{*n}, \tag{11}$$

$$\beta^* p^*(\beta^*)=11.69+\sum_{n=0}^{3} a_n \beta^{*n+1}/(n+1). \tag{12}$$

$NpT$-MC simulations were then performed at each value of $\beta^*$ using the appropriate value of $\beta^* p^*$ obtained from Eq. (12). The fit to the rhs of Eq. (7) was then updated, and the process iterated until the values of $\beta^* p^*$ at coexistence converged to within a desired tolerance of 1%. In practice, this only took one extra iteration after the initial integration using a predictor-corrector algorithm. In the current application, fluid-solid coexistence within a single simulation cell containing $O(10^2)$ particles is precluded by the free energy associated with forming an interface. Therefore, the fluid-phase and solid-phase simulations required to evaluate the rhs of Eq. (7) need not be coupled in any way to allow for, or forbid, a simulation spontaneously changing phase [25].

## III. SECOND-ORDER THERMODYNAMIC PERTURBATION THEORY

Phase diagrams were computed using the STPT formulated by Barker and Henderson [13–15]. The total Helmholtz free energy per particle, in units of $k_{\rm B}T$, is written as the sum of the hard-sphere contribution $\beta f_0$, plus first- and second-order terms $\beta f_1$ and $\beta f_2$, respectively, arising from the attractive part of the interaction potential,

$$\beta f=\beta f_0+\beta f_1+\beta f_2. \tag{13}$$

The first-order term $O(\beta^*)$ is given in terms of the hard-sphere radial distribution function, $g_0(r)$, at the desired density by

$$\beta f_1=2\pi\rho\beta\int_d^{\infty} r^2 v_1(r) g_0(r) dr. \tag{14}$$

The second-order term $O(\beta^{*2})$ is given exactly by an integral involving the hard-sphere four-body correlation function. We employ Barker and Henderson's ''macroscopic compressibility'' approximation [13–15], in which $\beta f_2$ is given by

$$\beta f_2=-\pi\rho\beta^2\left(\frac{\partial\rho}{\partial\beta p}\right)_0\int_d^{\infty} r^2 v_1^2(r) g_0(r) dr, \tag{15}$$

where $(\partial\rho/\partial\beta p)_0$ is evaluated in the reference hard-sphere system.

The thermodynamic and structural properties of the reference hard-sphere system are well known. We use the

Carnahan-Starling expressions for the hard-sphere fluid free energy and equation of state [19],

$$\beta f_0 = \frac{\eta(4-3\eta)}{(1-\eta)^2}, \tag{16}$$

$$\frac{\beta p_0}{\rho} = \frac{1+\eta+\eta^2-\eta^3}{(1-\eta)^3}, \tag{17}$$

$$\left(\frac{\partial\rho}{\partial\beta p}\right)_0 = \frac{(1-\eta)^4}{1+4\eta+4\eta^2-4\eta^3+\eta^4}, \tag{18}$$

where $\eta=\pi\rho^*/6$ is the packing fraction. The fluid-phase radial distribution function, $g_0(r)$, was obtained as prescribed by Verlet and Weis [22].

For the thermodynamic properties of the hard-sphere (fcc) solid, we use the expressions given by Alder *et al.* [20],

$$\beta f_0 = \ln\rho_0^* + 3\ln\left(\frac{3}{2\alpha}\right) - S_0 - S_1\alpha - S_2\alpha^2, \tag{19}$$

$$\frac{\beta p_0}{\rho} = \frac{3}{\alpha} + C_0 + C_1\alpha, \tag{20}$$

$$\left(\frac{\partial\rho}{\partial\beta p}\right)_0 = \left(\frac{3}{\alpha^2} + \frac{6}{\alpha} + C_0 - C_1\right)^{-1}, \tag{21}$$

in which the coefficients $S_0$, $S_1$, $S_2$, $C_0$, and $C_1$ are listed in Ref. [20], $\rho_0^*=\sqrt{2}$ is the close-packed density, and $\alpha=(\rho_0^*-\rho^*)/\rho^*$. The radial distribution function of the hard-sphere fcc solid was calculated using the expressions given by Kincaid and Weis [23].

Once the Helmholtz free energy is known, all other thermodynamic functions follow. The conditions for coexistence between phases 1 and 2 are $T_1=T_2$, $p_1=p_2$, and $\mu_1=\mu_2$. The latter two quantities can be obtained using the thermodynamic relationships

$$\frac{\beta p}{\rho} = \rho\left(\frac{\partial\beta f}{\partial\rho}\right), \tag{22}$$

$$\beta\mu = \beta f + \frac{\beta p}{\rho}. \tag{23}$$

## IV. VAN DER WAALS THEORY

One way of generating an augmented van der Waals theory is to set $\beta f_2=0$ in Eq. (13), and to evaluate Eq. (14) assuming that $g_0(r)=1$ $(r\geqslant d)$. The first-order term in the Helmholtz free energy can therefore be approximated by

$$\beta f_1 = 2\pi\rho\beta\int_d^\infty r^2 v_1(r)dr, = -2\pi\rho^*\beta^*/\sigma. \tag{24}$$

The hard-sphere thermodynamic properties and phase coexistence are obtained as in the preceding section. We note that the phase diagram is characterized in terms of a reduced measure of temperature, $\beta^*/\sigma=1/\sigma T^*$, and hence the phase diagrams of systems with different potential-range parameters can be obtained by a trivial scaling of temperature; the density remains unchanged. For instance, the critical temperature and density, obtained by solving $(\partial p/\partial\rho)_T=0$ and $(\partial^2 p/\partial\rho^2)_T=0$ simultaneously, are

$$\sigma T_c^* = 1.131944\cdots, \tag{25}$$

$$\rho_c^* = 0.249129\cdots. \tag{26}$$

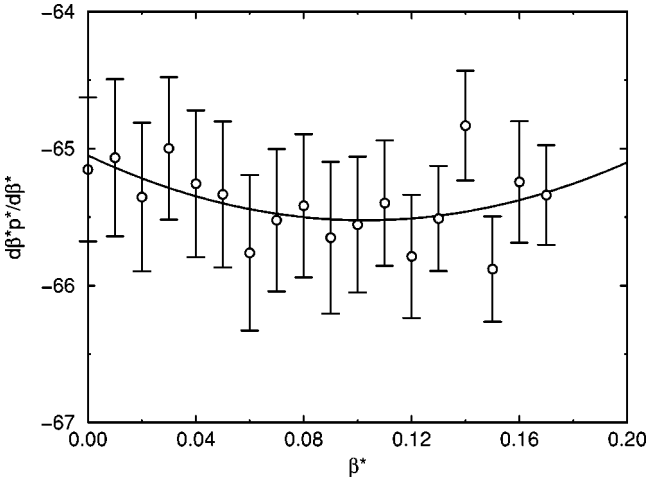


FIG. 1. $d\beta^*p^*/d\beta^*$ along the fluid-solid coexistence line for the system with $\sigma=0.1$: MC simulation (circles); cubic polynomial fit [Eq. (11)] (solid line).

## V. RESULTS

We have computed the phase diagrams of systems with $\sigma=0.1$, 1, and 3 using $NpT$-MC simulations, STPT, and van der Waals theory. In each case we present fluid-solid coexistence results obtained using the Gibbs-Duhem integration technique; vapor-liquid coexistence data are taken from Ref. [10]. For completeness, we also present phase diagrams for systems with $\sigma=4$, 5, and 6, calculated using STPT.

### A. $\sigma=0.1$

Simulation results from Gibbs-Duhem integration along the fluid-solid coexistence line for the system with $\sigma=0.1$ are shown in Figs. 1, 2, and 3. In Fig. 1, $d\beta^*p^*/d\beta^*$ [Eq. (7)] is plotted as a function of reciprocal temperature. Also shown is the cubic polynomial fit defined in Eq. (11). We note that the relative variation of this quantity is small $(<1\%)$ over the reciprocal temperature range $0\leqslant\beta^*\leqslant0.2$. In Fig. 2 we plot $\beta^*p^*$ at fluid-solid coexistence, along with the integrated fit [Eq. (12)]. The variation of $\beta^*p^*$ with $\beta^*$ is approximately linear. An estimate of the triple temperature, $T_t^*$ was obtained by extrapolating the simulation results to $\beta^*p^*=0$. Of course, the pressure and temperature at the triple point are finite, but the ratio $p^*/T^*$ is clearly very small, at least compared its value at infinite temperature. An approximate value for the triple temperature is therefore $T_t^*\simeq5.589$.

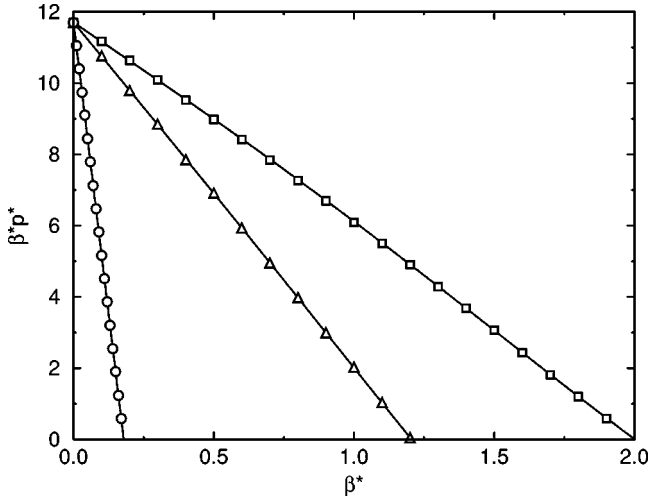


FIG. 2. $\beta^* p^*$ along the fluid-solid coexistence lines for the systems with $\sigma=0.1$ (circles), $\sigma=1$ (triangles), and $\sigma=3$ (squares). The solid lines are fits according to Eqs. (11) and (12).

The phase diagram for the system with $\sigma=0.1$ is shown in Fig. 3. Of the simulation results, the fluid-solid points are from the present work, and the vapor-liquid coexistence data are taken from Ref. [10]. Also shown in Fig. 3 are the theoretical phase diagrams calculated using STPT and van der Waals theory. The figure clearly shows that both STPT and van der Waals theory provide excellent descriptions of the simulation results. Critical-point and triple-point parameters from simulation and theory are summarized in Table I. A comparison of simulation and theory shows that there is very little to choose between STPT and van der Waals theory. Coincidentally, the simulation estimate of the critical temperature, $T_c^*=11.452$ lies exactly half-way between the STPT and van der Waals theory results of 11.585 and 11.319, respectively. Mean-field theories predict an order-parameter critical exponent of $\beta=\frac{1}{2}$, which is appropriate for a system with $\sigma<3/2$ in three dimensions [2–6]. The success of the theories in describing the simulation results with $\sigma=0.1$ is due to the fact that the fluid structure (over length scales of a few sphere-diameters) is largely dictated by the hard-core repulsions, and is relatively insensitive to the presence of additional slowly varying long-range interactions. Moreover, a significant proportion of the configurational energy arises from interactions between particles at large separations, which means that it is not essential for a theory to describe accurately the short-range correlations of the system. Even for the solid phase, in which $g_0(r)$ retains structure at all distances, the approximation $g_0(r)=1$ leads to accurate results as compared to the simulations.

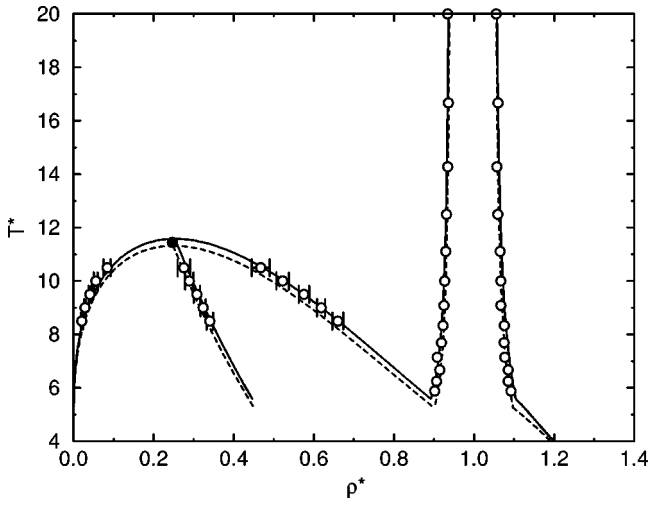


FIG. 3. Phase diagram in the $\rho^*$-$T^*$ plane for the system with $\sigma=0.1$: MC simulation (circles); second-order thermodynamic perturbation theory (solid lines); van der Waals theory (dashed lines). The fluid-solid simulation points are from the current work; the vapor-liquid simulation points are from Ref. [10].

### B. $\sigma=1$

Simulation results from Gibbs-Duhem integration along the fluid-solid coexistence line for the system with $\sigma=1$ are shown in Figs. 2, 4, and 5. Figure 4 contains $d\beta^* p^*/d\beta^*$ as a function of $\beta^*$, and shows that some curvature may occur in the plot of $\beta^* p^*$ against $\beta^*$. The latter is shown in Fig. 2, but the curvature is hardly discernible from the plot. By extrapolating the line to $\beta^* p^*=0$, as before, we obtain an estimate of the triple-point temperature $T_t^* \simeq 0.830$.

The phase diagram for the system with $\sigma=1$ is shown in Fig. 5. As before, simulation data for the vapor-liquid coexistence envelope are taken from Ref. [10]. Figure 5 shows that STPT provides a good description of vapor-liquid coexistence, but is only moderately successful in locating the fluid-solid phase boundaries. The van der Waals theory performs poorly in comparison with STPT. Critical-point and triple-point parameters from simulation and theory are summarized in Table I, and underline the superiority of STPT over van der Waals theory in describing the simulation results. Mean-field theories predict an order-parameter critical exponent of $\beta=\frac{1}{2}$, which is appropriate for a system with $\sigma<3/2$ in three dimensions [2–6]. Clearly, the approximations made in the van der Waals theory are unjustified for the potential with $\sigma=1$. Account has to be taken of the short-range correlations between the particles, which the STPT achieves through use of the hard-sphere radial distribution function, $g_0(r)$.

### C. $\sigma=3$

Simulation results from Gibbs-Duhem integration along the fluid-solid coexistence line for the system with $\sigma=3$ are shown in Figs. 2, 6, and 7. Figure 6 shows that there should be some discernible curvature in the plot of $\beta^* p^*$ against $\beta^*$, and Fig. 2 shows this to be the case. Extrapolating the curve in Fig. 2 to $\beta^* p^*=0$ yields an estimate of the triple-point temperature of $T_t^*=0.500$.

The phase diagram for the system with $\sigma=3$ is shown in Fig. 7. Simulation data for the vapor-liquid coexistence envelope are taken from Ref. [10]. STPT is seen to provide a reasonably accurate description of the simulation results. Critical-point and triple-point parameters from simulation and theory are summarized in Table I. STPT overestimates

TABLE I. Critical-point and triple-point parameters from Monte Carlo (MC) simulation, second-order thermodynamic perturbation theory (STPT), and van der Waals (vdW) theory. MC estimates of the vapor-liquid critical parameters are taken from Ref. [10]. Figures in parentheses are estimated statistical uncertainties in the last digit.

| Method | $T_c^*$ | $\rho_c^*$ | $T_t^*$ | $\rho_t^*$(vap) | $\rho_t^*$(liq) | $\rho_t^*$(sol) |
|---|---|---|---|---|---|---|
| | | | $\sigma=0.1$ | | | |
| MC | 11.452(8) | 0.247(5) | 5.589 | | | |
| STPT | 11.585 | 0.252 | 5.585 | 0.000812 | 0.892 | 1.104 |
| vdW | 11.319 | 0.249 | 5.260 | 0.000563 | 0.901 | 1.098 |
| | | | $\sigma=1$ | | | |
| MC | 1.3724(1) | 0.2993(1) | 0.830 | | | |
| STPT | 1.3834 | 0.2857 | 0.863 | 0.00709 | 0.836 | 1.127 |
| vdW | 1.1319 | 0.2491 | 0.526 | 0.000563 | 0.901 | 1.098 |
| | | | $\sigma=3$ | | | |
| MC | 0.5972(1) | 0.3757(4) | 0.500 | | | |
| STPT | 0.6221 | 0.4143 | 0.532 | 0.0757 | 0.751 | 1.152 |
| vdW | 0.3773 | 0.2491 | 0.175 | 0.000563 | 0.901 | 1.098 |
| | | | $\sigma=4$ | | | |
| STPT | 0.5341 | 0.4815 | 0.494 | 0.181 | 0.700 | 1.165 |
| | | | $\sigma=5$ | | | |
| STPT | 0.4822 | 0.5183 | 0.473 | 0.390 | 0.617 | 1.180 |
| | | | $\sigma=6$ | | | |
| STPT | 0.4447 | 0.5377 | | | | |

$T_c^*$ and $T_t^*$ by about 10% and 6%, respectively. The van der Waals theory predicts $T_c^*=0.3773$, and so for the sake of clarity the phase diagram has been omitted from the figure. Mean-field theories predict an order-parameter critical exponent of $\beta=\frac{1}{2}$, whereas for short-range interactions the correct (Ising) exponent is $\beta=0.326(4)$ [1]. As for $\sigma=1$, a poor description of the short-range correlations in this system compromises the performance of the van der Waals theory. The accuracy of STPT is diminished slightly because at low temperatures the effect of short-range interactions on the fluid structure is more pronounced; the attractions no longer arise from a slowly varying potential between the particles.

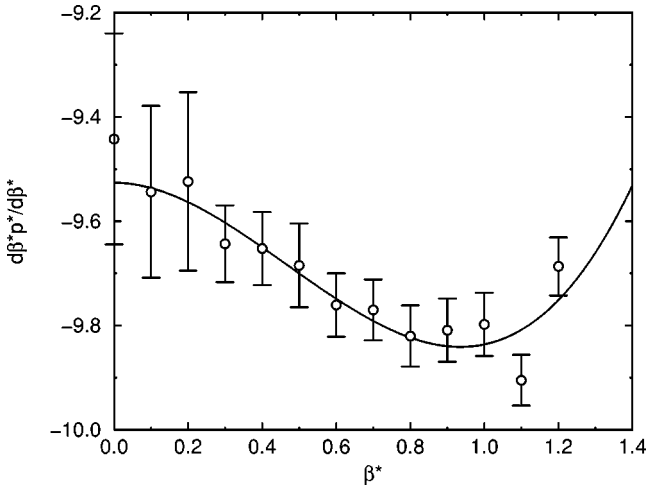


FIG. 4. $d\beta^* p^*/d\beta^*$ along the fluid-solid coexistence line for the system with $\sigma=1$: MC simulation (circles); cubic polynomial fit [Eq. (11)] (solid line).

### D. $\sigma=4-6$

In the previous sections we have shown that STPT provides reasonably accurate predictions for the phase diagrams of systems with $\sigma\leqslant 3$, whereas the van der Waals theory fares badly with short-range potentials ($\sigma\geqslant 1$). We have therefore used STPT to calculate the phase diagrams of systems with $\sigma=4$, 5, and 6, which are shown in Figs. 8, 9, and 10, respectively. As the range of the potential is decreased, the vapor-liquid critical temperature decreases with respect to the triple-point temperature, until at $\sigma=6$ the en-

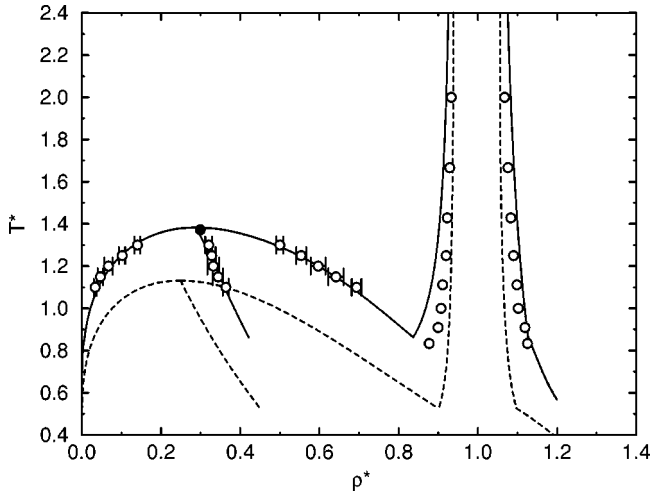


FIG. 5. Phase diagram in the $\rho^*$-$T^*$ plane for the system with $\sigma=1$: MC simulation (circles); second-order thermodynamic perturbation theory (solid lines); van der Waals theory (dashed lines). The fluid-solid simulation points are from the current work; the vapor-liquid simulation points are from Ref. [10].

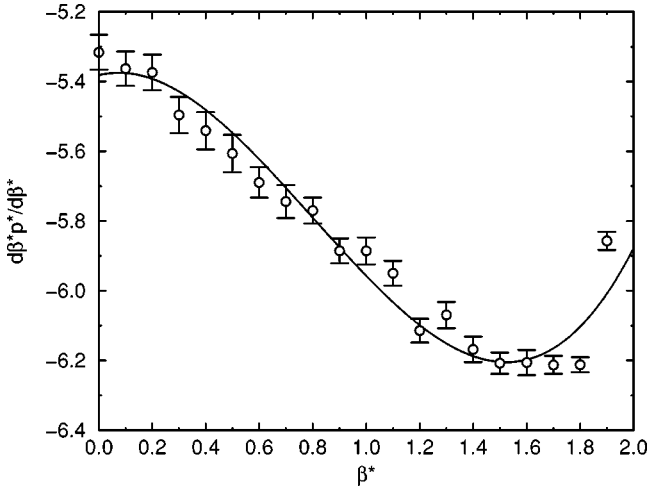


FIG. 6. $d\beta^* p^*/d\beta^*$ along the fluid-solid coexistence line for the system with $\sigma=3$: MC simulation (circles); cubic polynomial fit [Eq. (11)] (solid line).

tire vapor-liquid coexistence envelope is contained within the fluid-solid coexistence boundaries. Critical-point and triple-point parameters from STPT are presented in Table I.

The vapor-liquid transition becomes metastable with respect to freezing when $\sigma \gtrsim 5$. This result is in broad agreement with that for the hard-core attractive Yukawa system [26]. We can make a link between the potential in Eq. (3), and the Yukawa potential $v_1(r) = -\epsilon \exp[-\kappa(r-d)](d/r)$, by calculating the effective interaction strength $\epsilon_{\text{eff}}$ as being proportional to $\int_d^\infty r^2 v_1(r) dr$. For the Yukawa potential we get $\epsilon_{\text{eff}} \propto (\kappa d+1)/(\kappa d)^2$, and for the potential in Eq. (3) we get $\epsilon_{\text{eff}} \propto 1/\sigma$. Equating these expressions gives an approximate mapping between the two range parameters. On the basis that vapor-liquid coexistence becomes metastable with respect to freezing for the attractive Yukawa system when $\kappa d \gtrsim 6$ [26], we should expect the same to occur for the potential in Eq. (3) when $\sigma \gtrsim 36/7 = 5.14\ldots$; this is entirely consistent with the results from STPT obtained in the present work.

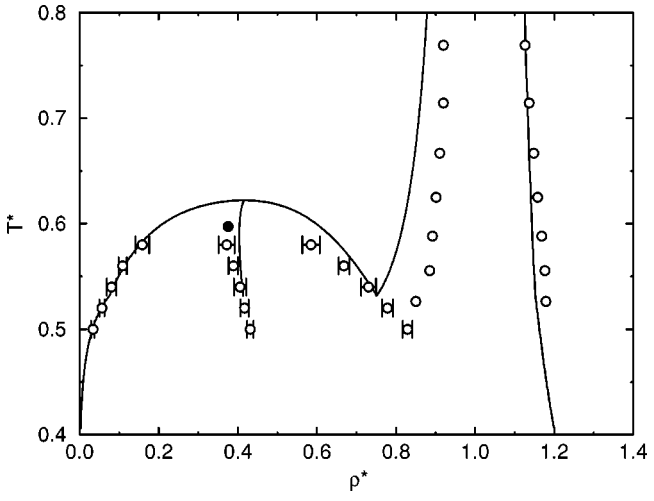


FIG. 7. Phase diagram in the $\rho^*$-$T^*$ plane for the system with $\sigma=3$: MC simulation (circles); second-order thermodynamic perturbation theory (solid lines). The fluid-solid simulation points are from the current work; the vapor-liquid simulation points are from Ref. [10].

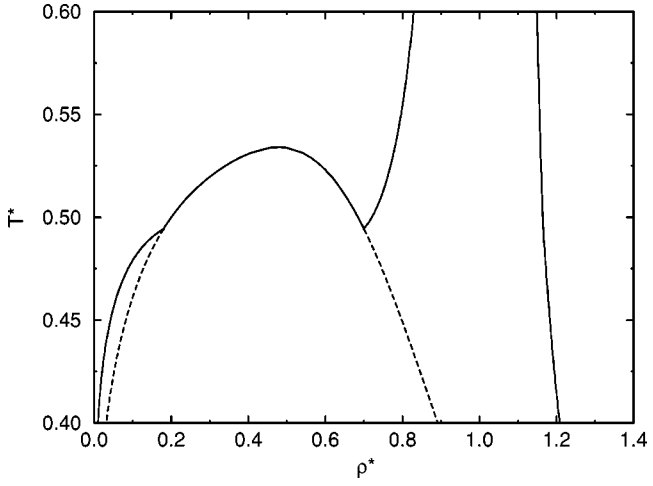


FIG. 8. Phase diagram in the $\rho^*$-$T^*$ plane for the system with $\sigma=4$ from second-order thermodynamic perturbation theory. The dashed lines indicate where vapor-liquid coexistence is metastable with respect to freezing.

## VI. CONCLUSIONS

In this paper we have calculated phase diagrams of systems consisting of hard spheres interacting with algebraically decaying attractive interactions, using Monte Carlo simulations, second-order perturbation theory, and an augmented van der Waals theory. The main aims of this study were: to assess the performance of mean-field theories in describing the phase boundaries obtained from high-accuracy simulations of systems with long-range interactions; to locate at which point the interactions becomes so short ranged that the vapor-liquid transition becomes metastable with respect to freezing.

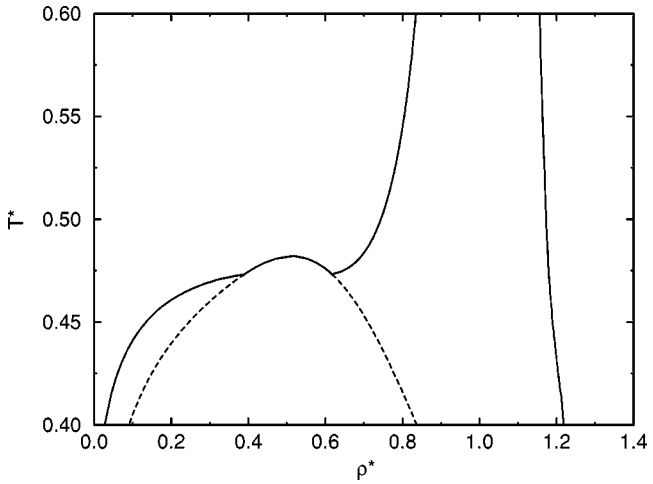


FIG. 9. Phase diagram in the $\rho^*$-$T^*$ plane for the system with $\sigma=5$ from second-order thermodynamic perturbation theory. The dashed lines indicate where vapor-liquid coexistence is metastable with respect to freezing.

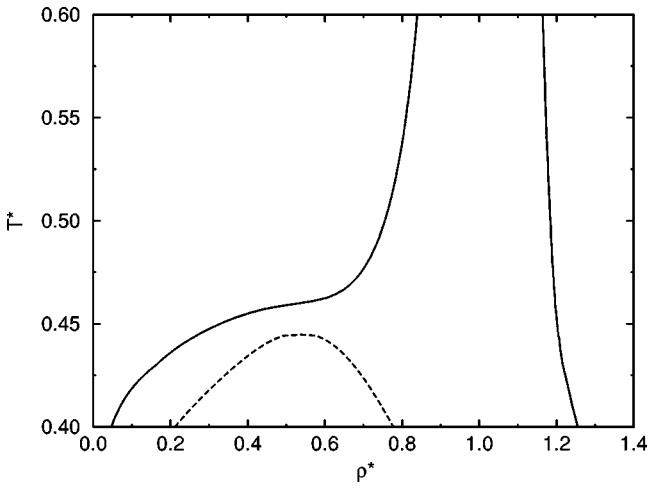


FIG. 10. Phase diagram in the $\rho^*$-$T^*$ plane for the system with $\sigma=6$ from second-order thermodynamic perturbation theory. The dashed lines indicate that the vapor-liquid transition is metastable with respect to freezing.

A comparison of simulation and theoretical phase diagrams, and associated critical-point and triple-point parameters, shows that while second-order perturbation theory and van der Waals theory are very accurate when the potential is long ranged ($\sigma=0.1$), they perform less well when the range of potential is decreased ($\sigma=1$ and 3). This can be put down to the fact that in systems with short-range potentials, the short-range correlations are significant in determining the overall thermodynamics. By contrast, in systems with long-range potentials, a larger contribution to the overall configurational energy, and hence free energy, arises from interactions between pairs of particles that are so far removed from one another that their relative positions are uncorrelated. Hence, it is more important to describe the short-range correlations accurately for systems with short-range potentials than it is for systems with long-range potentials. Accordingly, for $\sigma=1$ and 3, second-order perturbation theory is seen to be more reliable than the augmented van der Waals theory.

Phase diagrams for systems with shorter-range potentials ($\sigma=4$, 5, and 6), calculated using second-order perturbation theory, indicate that the vapor-liquid transition becomes metastable with respect to freezing when $\sigma\gtrsim 5$. This is in broad agreement with simulation results for the hard-core attractive Yukawa system [26], which indicate that vapor-liquid coexistence disappears from the equilibrium phase diagram when $\kappa d\gtrsim 6$. An approximate mapping between the Yukawa potential and the potential studied in this work shows that these criteria are, to some extent, equivalent.

[1] A.M. Ferrenberg and D.P. Landau, Phys. Rev. B **44**, 5081 (1991).
[2] G. Stell, Phys. Rev. B **1**, 2265 (1970).
[3] M.E. Fisher, S. Ma, and B.G. Nickel, Phys. Rev. Lett. **29**, 917 (1972).
[4] G. Stell, Phys. Rev. B **8**, 1271 (1973).
[5] M. Aizenman and R. Fernández, Lett. Math. Phys. **16**, 39 (1988).
[6] J. Sak, Phys. Rev. B **8**, 281 (1973).
[7] R. Guida and J. Zinn-Justin, J. Phys. A **31**, 8103 (1998).
[8] E. Luijten and H.W.J. Blöte, Phys. Rev. Lett. **89**, 025703 (2002).
[9] E. Luijten and H.W.J. Blöte, Phys. Rev. B **56**, 8945 (1997).
[10] P.J. Camp and G.N. Patey, J. Chem. Phys. **114**, 399 (2001).
[11] N.V. Brilliantov and J.P. Valleau, J. Chem. Phys. **108**, 1123 (1998).
[12] L. Vega, E. de Miguel, L.F. Rull, G. Jackson, and I.A. McLure, J. Chem. Phys. **96**, 2296 (1992).
[13] J.A. Barker and D. Henderson, J. Chem. Phys. **47**, 2856 (1967).
[14] J.A. Barker and D. Henderson, J. Chem. Phys. **47**, 4714 (1967).
[15] J.A. Barker and D. Henderson, Rev. Mod. Phys. **48**, 587 (1976).
[16] B. Widom, J. Chem. Phys. **39**, 2808 (1963).
[17] H.C. Longuet-Higgins and B. Widom, Mol. Phys. **8**, 549 (1964).
[18] J.-P. Hansen and I. R. McDonald, *Theory of Simple Liquids* (Academic Press, London, 1986).
[19] N.F. Carnahan and K.E. Starling, J. Chem. Phys. **51**, 635 (1969).
[20] B.J. Alder, W.G. Hoover, and F.H. Ree, J. Chem. Phys. **49**, 3688 (1968).
[21] R. Hall, J. Chem. Phys. **57**, 2252 (1972).
[22] L. Verlet and J.J. Weis, Phys. Rev. A **5**, 939 (1972).
[23] J.M. Kincaid and J.J. Weis, Mol. Phys. **34**, 931 (1977).
[24] A.D. Bruce, A.N. Jackson, G.J. Ackland, and N.B. Wilding, Phys. Rev. E **61**, 906 (2000).
[25] D.A. Kofke, J. Chem. Phys. **98**, 4149 (1993).
[26] M.H.J. Hagen and D. Frenkel, J. Chem. Phys. **101**, 4093 (1994).
[27] P. Bolhuis, M. Hagen, and D. Frenkel, Phys. Rev. E **50**, 4880 (1994).
[28] G. Foffi, G.D. McCullagh, A. Lawlor, E. Zaccarelli, K.A. Dawson, F. Sciortino, P. Tartaglia, D. Pini, and G. Stell, Phys. Rev. E **65**, 031407 (2002).
[29] P. Bolhuis and D. Frenkel, Phys. Rev. Lett. **72**, 2211 (1994).
[30] P. Germain and S. Amokrane, Phys. Rev. E **65**, 031109 (2002).
[31] D.M. Heyes and L.V. Woodcock, Mol. Phys. **59**, 1369 (1986).
[32] J. Largo and J.R. Solana, Int. J. Thermophys. **21**, 899 (2000).
[33] M.G. Noro, N. Kern, and D. Frenkel, Europhys. Lett. **48**, 332 (1999).
[34] M. P. Allen and D. J. Tildesley, *Computer Simulation of Liquids* (Clarendon Press, Oxford, 1987).
[35] W.G. Hoover and F.H. Ree, J. Chem. Phys. **49**, 3609 (1968).